



Sharif University of Technology
Scientia Iranica
Transactions B: Mechanical Engineering
www.scientiairanica.com



Research Note

An efficient three-axis numerically controlled rough-cutting machining approach on five-axis machine for an integral centrifugal impeller

Y. Chen^a, G.F. Mei^a, J.B. Wang^b, C.Y. Yao^b and J. Gao^{a,*}

a. School of Mechanical, Electrical, & Information Engineering, Shandong University at Weihai, Shandong, Postcode: 264209, China.

b. Shandong Shuanglun Co., Ltd., Weihai, China.

Received 21 November 2013; received in revised form 25 March 2015; accepted 16 April 2015

KEYWORDS

Centrifugal impeller;
Unit Machining
Regions (UMRs);
Simultaneous
three-axis NC
machining;
Five-axis machining;
Cutting simulation on
Vericut software.

Abstract. To improve the machining efficiency for the conventional five-axis Numerically Controlled (NC) machining of a centrifugal impeller, this paper presents an efficient simultaneous three-axis NC machining approach on five-axis machine instead of simultaneous five-axis NC machining technology. On the basis of the characteristic curves of an impeller and its projection graphs, the rough-cut surface of blades is partitioned into several Unit Machining Regions (UMRs). The rotating and tilting angles of a five-axis machine bed are calculated and fixed in advance to support the simultaneous three-axis NC machining of each UMR. Tool paths with a zigzag shape are generated to avoid interference and collision between the cutter and the impeller blades based on the simultaneous three-axis control approach on five-axis machine bed. A prototype model of an impeller with nine blades is established, and its final tool paths in each UMR are verified by means of a cutting simulation function on Vericut software. Simulation results demonstrate that the simultaneous three-axis machining approach on five-axis machine bed can significantly improve the machining efficiency compared to the conventional five-axis machining technology.

© 2015 Sharif University of Technology. All rights reserved.

1. Introduction

Centrifugal impeller is one type of complex component mainly used to compress or transfer fluid at high speed and high pressure. It has also been commonly applied in energy generators, aerospace, crafts, petrochemical industry, and so on [1,2]. An impeller consists of several complex multi-blades with sophisticated geometrical shapes and narrow flow channel hub surfaces, which will take a lot of time to remove the unnecessary material between two adjacent blades. Furthermore, lack of balance of an impeller due to its asymmetrical weights

and shapes can also make the impeller particularly subject to a great deal of breakage [3]. Hence, it will be very critical to improve the machining quality and efficiency of a centrifugal impeller by means of some advanced NC machining technologies.

Centrifugal impeller is, in general, manufactured as an integral shape on five-axis NC machine or by means of the lost-wax casting technology. The five-axis NC machine has been widely used to manufacture aerospace parts and turbine impellers with complex geometry. Compared to three-axis machining, the cutter axis of five-axis machine has two additional degrees of freedom allowing a more efficient tool path. Hence, five-axis machining can offer more advantages such as higher productivity and better machining

*. Corresponding author. Tel.: +86 631 5688220
E-mail address: shdgj@sdu.edu.cn (J. Gao)

quality than three-axis machining. The surface model of the impeller is very complex with extremely twisted surfaces and substantially overlapped blades. These complex surfaces make it ideally suitable for five-axis NC machining instead of three-axis machining, because flexible movements of the cutter axis can avoid collision or interference between the cutter and the work piece. However, five-axis machining method will spend more time removing the materials because of its complex multi-axis control and large processing volume. To improve the machining efficiency and quality of the centrifugal impeller, this paper will present an efficient simultaneous three-axis control scheme on a five-axis NC machine instead of a simultaneous five-axis control method. In the simultaneous three-axis control scheme, two rotational DOFs on five-axis NC machine are fixed to make the cutter axis be perpendicular to the machined region, and then the region can be cut by means of the simultaneous three-axis control method on three-axis NC machine.

Most five-axis machining technologies of the centrifugal impeller have been devoted to avoid the collision and interference between the blade and the cutter, and to improve the machining quality by means of the tool path plan. For example, Fan et al. [4] developed a novel five-axis tool positioning algorithm for open concave surface machining. Chaves et al. [5] dealt with improvement of the machining quality of impeller blades based on evaluation of the geometric and economical performances of a tool path. Jung et al. [6] developed a tool path plan method of an impeller with high machining efficiency and excellent surface quality by means of a B-spline function on five-axis machine. Feng et al. [7] presented a novel assigning tool orientations method to produce smooth and interference-free tool orientation for the five-axis machining of an impeller. Chen et al. [8] developed iso-scallop trajectories, tool orientations, and a tool swept volume for the five-axis machining of an impeller. Huang et al. [9] put forward many novel region partitioning methods through generation of the ruled envelope surfaces. Gong et al. [10] proposed a novel tool path generation method of flank milling based on the constraints of ball end cutters. Chu et al. [11] investigated a tool path planning method for five-axis flank milling of the ruled surfaces by means of NC linear interpolation. Some research has also been carried out to improve machining efficiency of the five-axis NC machine. Beudaert et al. [12] proposed an iterative approach to smooth an initial tool path by means of the kinematical constraints of tool path, such as the maximum velocity, acceleration, and jerk. Beudaert et al. [13] presented an indicator of the maximum feed rate to smooth the tool paths and reduce the machining time of five-axis machining. In order to find the complicated engagement between cutter and work

piece, Layegh et al. [14] established an enhanced force model based on the feed rate scheduling technique for rough-cut of parts.

However, most five-axis machining technologies for the centrifugal impeller have just solved the problems of avoidance of collision and interference and improvement of machining quality; no attention is paid to machining efficiency of the three-axis control method on five-axis NC machine in terms of machining time. As a matter of fact, a centrifugal impeller is composed of some complex multi-blade and narrow flow channel hub surfaces. Its machining efficiency has great influences on enlargement of its economical performances and machining quality. Moreover, most five-axis machining technologies sacrifice machining efficiency to improve machining quality, or avoid the collisions or interferences between the cutter axis and the blade. Especially, these parametric cutting methods for the machining of blade surfaces is likely to decrease the rate of metal removal since it has to control all the five axes coordinately to trace the tool path. Hence, to improve machining efficiency, this paper will present a simultaneous three-axis control scheme for the centrifugal impeller on five-axis machine instead of the simultaneous five-axis control method.

This paper is organized into six sections. Following the introduction, Section 2 addresses some preliminaries and region partitioning of a centrifugal impeller, which consists of the surface model of a centrifugal impeller, determination of the cutter axis and region partitioning method. Section 3 is devoted to generate the tool path in rough-cut. In Section 4, some simulation results are illustrated on feasibility of the proposed simultaneous three-axis NC machining method on five-axis machine through computer cutting simulation on Vericut software. Some conclusion remarks are finally included in Section 5.

2. Preliminaries and UMRs region partitioning of an impeller

The centrifugal impeller, shown in Figure 1(a), is a circular revolving entity. It is composed of nine identical blades and a hub. The angle variation value between the adjacent two blades is equal to 40° . The surface model of a centrifugal impeller can be separated into two parts: the blades and the hub. As shown in Figure 1(a), every blade of an impeller consists of a suction surface, a pressure surface, a leading edge, and a trailing edge. The hub surface is generated by revolving the hub curve about the rotating axis of the impeller. The shroud surface identifies the outer shape of the blade. The surface of the blade is closed among the shroud surface, suction surface, and pressure surface. Rotating the shroud curve around the axis of rotation forms the shroud surface.

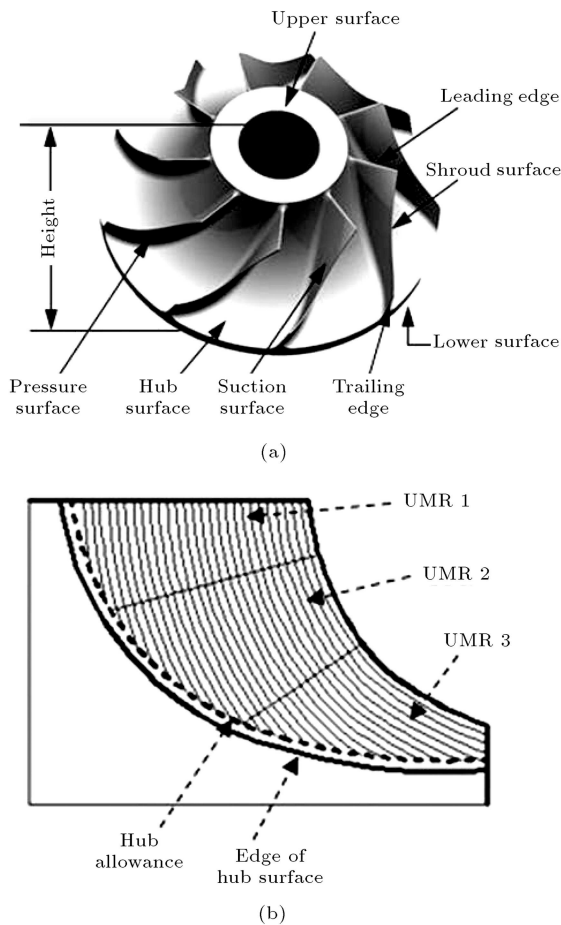


Figure 1. Surface model of a centrifugal impeller: (a) Geometric features; and (b) UMRs rough-cut regions.

2.1. UMRs region partitioning of a centrifugal impeller

To reduce the point contact time of a cutter, a blade shape consisting of straight-line elements on the pressure and suction surfaces is preferred to make the cutter having a line contact with the impeller. In this way, a geometric model of a centrifugal impeller, in Figure 1(a), has been developed based on canonical representations in curvilinear coordinates. In addition, in order to avoid the collisions or interferences between

the cutter axis and the blade, the rough-cut surface of each blade is partitioned into several UMRs shown in Figure 1(b).

In each UMR, the direction of the cutter is used for machining of the unit machining regions. The rotating and tilting axes in a machine bed have to be set up in advance for each UMR in order for the UMR to be milled by the three-axis machining manner. The representative ruling vectors of the pressure and suction surfaces are used to determine the rotating and tilting angles of a machine bed. An arbitrary ruling vector is selected on the ruled surface of a blade to coincide with the cutter axis vector that has to correspond to the vertical or horizontal axis of a machine spindle. Then, the feasible UMR that is accessible by the tool can be determined by the projection curves obtained through a few rotational transformations, as shown in Figure 2(a)-(c). The ruling vector is sequentially transformed by rotation about the x -axis and Y -axis of angles α and β , respectively. As shown in Figure 2(b) and (c), the values of α and β are equal to the angles between the ruled line vectors and the $x - z$ plane, $y - z$ plane, respectively. After these rotation transformations are completed, the roughing areas are projected onto the $x - y$ plane.

Figure 3 demonstrates that the shaded area is the interference-free region in which the cutter, having a fixed cutter axis vector, can move on the hub surface without collision with the impeller blades. As shown in Figure 3, the appropriate UMRs can be

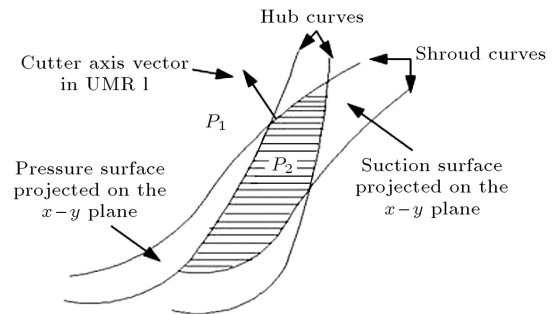


Figure 3. Blade contour projected on the $x - y$ plane.

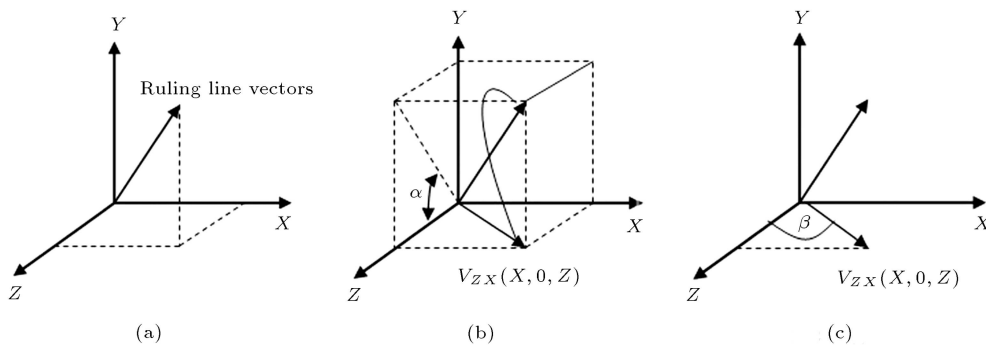


Figure 2. Determination of the direction of cutter axis: (a) Ruled line vectors; (b) rotation about the x -axis; and (c) rotation about the y -axis.

determined according to the intersection point between the adjacent hub curves and shroud curves. The cutter axis is coincided with the ruling line at point P_1 . A similar approach is proposed for constructing the next UMR and cutter axis by examining the angles of α and β . Hence, all of the UMRs and the cutter axis can be determined. The rotating and tilting angles of a machine bed can be computed by the transformation angles of α and β , respectively.

Machining area partitioning means that a machining area on a hub surface is divided into a certain number of UMRs, each of which is to be machined by the three-axis machining without any collision between the cutter and the blade surfaces. On the basis of this region partitioning, this paper designs a detailed procedure of machining area partitioning shown in Figure 4. Firstly, the geometry framework of integral impeller and blank information can be obtained according to the CAD database of the centrifugal impeller. And then, some characteristic curves of the impeller, such as the edge of blade surface curves and hub surface curves need to be found out from the geometric data of the impeller. The ruling vectors used for the fixed cutter axes are then calculated. To obtain the first UMR, the first ruling vector on the shroud curve of the suction surface is assigned as the fixed cutter axis, and the point P_1 is set to the upper boundary point shown in Figure 3. The assigned

ruling vector is transformed by rotation about the x -axis and y -axis of angles α and β to coincide with the z -axis. The shroud and hub curves are projected onto the $x - y$ plane to determine the boundary of each feasible machining area. If an intersection point appears between the opposite shroud curve and the hub curve of the ruling vector, the intersection point, P_2 , is set to the lower boundary point, the first partitioned region is saved as UMR, and the next cutter axis vector is assigned to obtain the next UMR. If the point P_2 is the last point in the ruling lines of the blades surface, the last point of the opposite shroud curve is set to the lower boundary point, and the partitioning procedure ends. Otherwise, $P_1 = P_2$, $NO_{UMR} = NO_{UMR} + 1$, and get to the third step; finally, all the UMRs and tool axes are obtained and saved.

2.2. Determination of the direction for cutter axis

Rational selection of geometry parameter of the cutter is very important to raise processed quality. To improve the manufacturing efficiency, it is desirable to select a cutter with a large size; however, too large size tends to result in interference or collision between the cutter and the impeller blades. For isometric blades of impeller, the iterative method proposed by Layegh [14] will be applied to calculate the shortest distance (d_{min}) between two adjacent blades. To avoid collision and interference between the cutter and the impeller blades, a protection factor, k , is chosen as $1.2 < k < 1.5$, hence, maximum radius of the ball end milling cutter is designed as follows.

$$r_{max} = \frac{d_{min} - 2\eta}{2k}, \tag{1}$$

where η denotes the finishing allowance, and the radius of the cutter can be selected as $r < r_{max}$.

Directions of the cutter axis at points P_i ($i = 1, 2, \dots, n$) are demonstrated in Figure 5. The pressure surface of each blade is manufactured by means of an isometric or Cartesian method proposed by Jung [6]. Thus, the cutter axis is coincided with the ruling line at point P_1 . As shown in Figure 5, $P_{S,i}$ and $P_{X,i}$ ($i = 1, 2, \dots, n$) denote the points on the shroud curve and the hub curve. For a given maximum cutting depth, l , the number of cutting layers can be calculated as $n_1 = L/l$ in which L is the length of ruling lines on the blade surface. Then, the position of cutter point at the j th line in the k th cutting layer can be calculated as follows:

$$O_{i,j,k} = O_{i,j,k-1} + \frac{(P_{s,i} - P_{x,i}) \times (n_1 - k)}{n_1}, \tag{2}$$

where $k = 1, 2, \dots, n_1$.

Direction of the cutter axis at the j th line in the

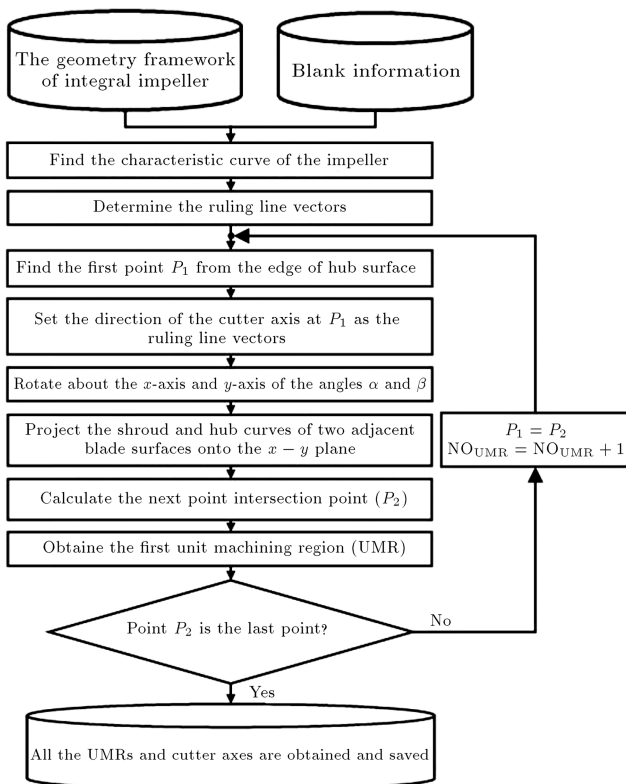


Figure 4. Flowchart of region partitioning based on the fixed cutter vectors.

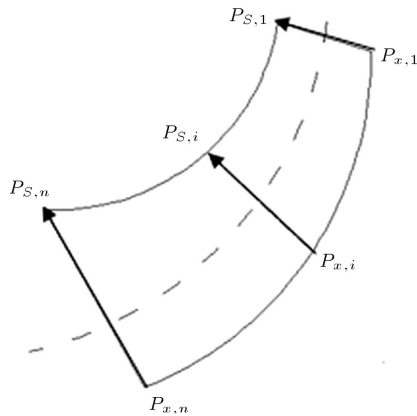


Figure 5. Determination of the direction for cutter axis.

k th cutting layer can be expressed as follows.

$$T_{i,j,k} = \frac{P_{s,i} - O_{i,j,k}}{\|P_{s,i} - O_{i,j,k}\|}, \quad (3)$$

where $O_{i,j,k}$ denotes the cutter point at the j th line in the k th cutting layer.

3. Generation of tool path in rough-cut

A cylindrical blank is first machined by means of lathe to form the outer profile of the shroud surface of an impeller. Then, rough-cut milling is performed on each UMR between two adjacent blade surfaces. Rough-cut milling or rough machining quickly removes unnecessary materials from this profiled blank and produces the pre-form of an impeller so as to facilitate the final finish cut. Thus, the tool path for rough-cut machining should be generated so that the metal removal rate can be maximized during the rough process without any collision or interference between the cutter and the impeller surfaces. The tool moves on each UMR in a series of zigzags, which can produce less number of tool paths and memory. Figure 6 illustrates the tool path with the shape of zigzags.

The cutting directions of adjacent two tool paths are opposite. The number of tool paths can be

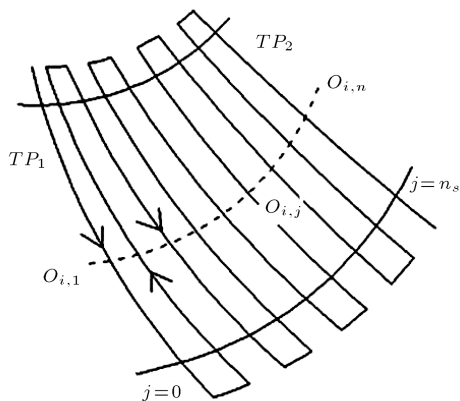


Figure 6. Tool path with the shape of zigzags.

calculated as follows:

$$n_s = \frac{S}{2\sqrt{d-h}}, \quad (4)$$

where S denotes the arc length between adjacent trailing edges, d is equal to the diameter of cutter, and h expresses the allowable value of residual height at the edge of hub surface.

As shown in Figure 6, the first tool path, TP_1 , is the intersection lines of the suction surface and the hub surface, and the last tool path, TP_2 , depends on the intersection between the pressure surface and the hub surface. These path points, $O_{i,j}$, on the tool path can be computed by means of the linear interpolation method.

$$O_{i,j} = O_{i,1} + \frac{O_{i,2} - O_{i,1}}{n_s} \cdot j, \quad (5)$$

where $j(j = 0, 1, \dots, n_s)$ denotes the number of lines on the tool path.

For rough-cut milling of a blade surface, the cutter has to mill the blade surface along the predefined tool path on the machining part surface. The tool path points on the hub surface at the side of the pressure surface can be determined based on the offset amount, by considering the blade allowance and the tool radius, as shown in Figure 7. Then, the first tool path on the hub surface at the side of the pressure surface, can be derived from blade allowance and tool radius, as follows:

$$OC_P(0) = \sum_{i=1}^{n-1} \{L_{P_{x,i}}(u) + d \cdot V_n(P_{x,i}(u)) + \delta \cdot V_T(j)\}, \quad (6)$$

where $L_{P_{x,i}}(u)$ denotes the i th hub curve at the edge of hub surface between $P_{x,i}$ and $P_{x,i+1}$ with $0 \leq u \leq 1$; $V_n(P_{x,i}(u))$ is the normal vector of $L_{p_{x,i}}(u)$ for a given i and u ; δ expresses the offset value from a hub curve along the tool axis vector; $V_T(j)$ denotes the tool axis vector of the j th UMRs; and d is equal to the offset values between two adjacent tool paths.

Meanwhile, the first tool path, $OC_S(0)$, at the side of the suction surface, can also be determined. Since the tool paths are uniformly distributed on the hub surface, the intersection angle between the adjacent two tool paths around the mid-axis of impeller has the same values, denoted as θ . Hence, the next tool path can also be determined as follows:

$$\begin{cases} OC_P(1) = R_z(\theta) \cdot OC_P(0) \\ OC_S(1) = R_z(\theta) \cdot OC_S(0) \end{cases} \quad (7)$$

Then, the i th tool path can also be calculated as follows:

$$\begin{cases} OC_P(i) = R_z(i\theta) \cdot OC_P(0) \\ OC_S(i) = R_z(i\theta) \cdot OC_S(0) \end{cases} \quad (8)$$

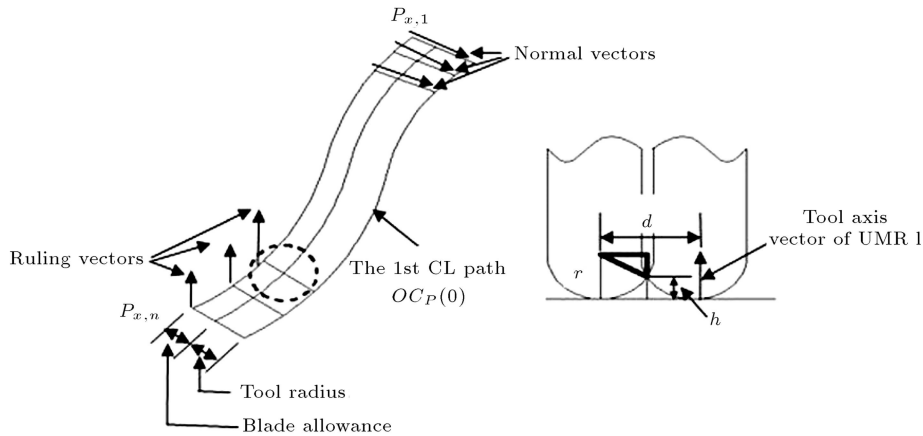


Figure 7. Tool path with blade allowance and tool radius.

where:

$$R_z(\theta) = \begin{bmatrix} \cos \theta & -\sin \theta & 0 \\ \sin \theta & \cos \theta & 0 \\ 0 & 0 & 1 \end{bmatrix},$$

and θ is equal to the angular value between the adjacent two tool paths around the mid-axis of impeller.

Furthermore, the general tool path, denoted as $TP(\theta_P)$, can be calculated by the two offset curves, $OC_P(\theta_P)$ and $OC_S(\theta - \theta_P)$, which are determined by rotating the first tool path, $OC_P(0)$ and $OC_S(0)$, around the mid-axis of impeller by θ_P and $\theta - \theta_P$, respectively. The final tool path $TP(\theta_P)$ can be expressed as follows:

$$TP(\theta_P) = (1 - \lambda).OC_P(\theta_P) + \lambda.OC_S(\theta - \theta_P), \quad (9)$$

where $\lambda = \frac{\theta_P}{\theta}$ is the interpolation ratio, and $0 \leq \lambda \leq 1$; θ_P is the rotation angle based on the path interval, and $0 \leq \theta_p \leq \theta$; θ denotes the angle between $OC_P(0)$ and $OC_S(0)$ around the mid-axis of the impeller.

It can be seen from Figure 8 that the tool path plane can easily be generated by extending the $TP(\theta_P)$ curves along the ruling lines. Thus, the final tool path of the cutter can be produced based on the $TP(\theta_P)$ curves. The number of cutting layers can be determined in terms of the milling depth a_p .

4. Numerical simulation and discussion

In order to verify the simultaneous three-axis NC manufacturing method on five-axis machine for an integral centrifugal impeller, a prototype rough-cut module of an impeller with nine blades, as shown in Figure 1, is established. According to the characteristic curves of an impeller and their projection graphs, the rough manufacturing module is partitioned into three UMRs by the blade contour projected on the $x - y$ plane. The rotating and tilting angles of a machine bed are calculated to support three-axis NC machining in

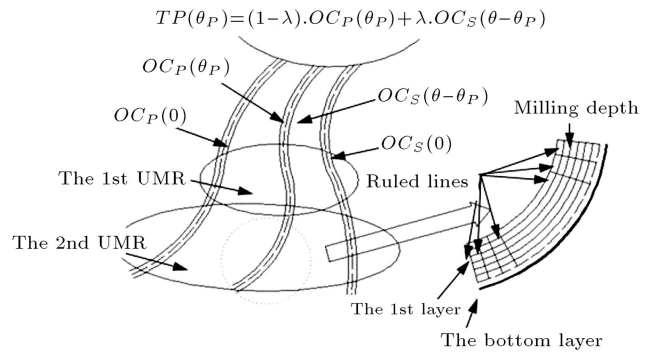


Figure 8. The initial offset tool path and a general tool path on the part surface.

each UMR. All accessible postures of the cutters at the ruling line are determined. Ball end mills with diameter of 10 mm are used successively in each UMR. An NC program for the generation of tool paths is first prepared by means of Automatically Programmed Tools (APT). Then, this program is transformed through the post-processing approach into a machine-specific code for a five-axis machining bed. The tool path with the characteristic of zigzag is generated based on the three-axis manufacturing plan at each UMR for the purpose of avoiding interference and collision between the tool and the impeller blades. The final tool paths of rough machining in each UMR are verified by means of the cutting simulation function of Vericut software.

For the purpose of comparing the machining efficiency of the simultaneous three-axis rough machining method with that of the conventional simultaneous five-axis machining approach, a lot of numerical simulations are conducted to measure the machining time. Table 1 demonstrates the rough-cut machining time of each UMR by means of the simultaneous three-axis and five-axis control at different feed rates of 500, 1000, 1500 and 2000 mm/min.

It can clearly be seen from Table 1 that the machining time by means of the simultaneous three-axis control is less than that by the simultaneous five-

Table 1. Comparison of rough-cut machining times: the simultaneous three-axis control versus five-axis control (time unit: min).

| Feed rates (mm/min) | | 500 | 1000 | 1500 | 2000 |
|------------------------------------|-------|--------|--------|--------|--------|
| Simultaneous three-axis control | UMR 1 | 25.654 | 12.975 | 8.749 | 6.644 |
| | UMR 2 | 16.201 | 8.254 | 5.605 | 4.285 |
| | UMR 3 | 17.262 | 8.729 | 5.885 | 4.469 |
| | total | 59.117 | 29.958 | 20.239 | 15.398 |
| Simultaneous five-axis control | | 66.169 | 33.447 | 22.389 | 16.882 |
| Increase of efficiency (%) | | 11.93 | 11.65 | 10.62 | 9.64 |

axis control. Meanwhile, as a result of the simultaneous three-axis control, its machining efficiency is increased much more than 10% compared to the simultaneous five-axis control method. As a matter of fact, the actual machining time takes much longer than the calculated nominal time due to the acceleration and deceleration effects of the NC machine controller.

5. Conclusion

To improve the machining efficiency of a centrifugal impeller, this paper presents an efficient rough-cut three-axis control approach by partitioning a rough machining area into several UMRs. In order to enable the three-axis machining of an impeller on a five-axis machine, the rotating and tilting angles of a machine bed are controlled in advance for certain setups. And, the rough-cut machining area is partitioned into smaller sub-areas to facilitate three-axis milling without any collision between the cutter and the blade surfaces in the sub-areas. A repetitive partitioning procedure is proposed to determine the partitioned UMRs by means of the projection graphs of shroud and hub curves. Then, the tool paths in each UMR are determined by using the simultaneous three-axis control approach on a five-axis machine bed, while any collision between the cutter and the impeller blades is prevented by maintaining the tool against the blade surface at an appropriate inclination angle.

A typical impeller with nine blades is established, and the final tool paths generated by the proposed method are verified by means of the cutting simulation function on Vericut software. The simulation results confirmed the increased efficiency in terms of machining time of the proposed three-axis control, rough-cut machining method. Further research will focus on the simultaneous three-axis control of other types of impellers.

Acknowledgments

This project is supported by National Natural Science Foundation of China (Grant No. 51375264), the

China Post-doctoral Science Foundation (Grant No. 2014T70632 and 2013M530318), and Research Awards Fund for Excellent Young and Middle-aged Scientists of Shandong Province (Grant No. BS2013ZZ008) and Post-doctoral innovation funds of Shandong Province (Grant No. 201303105).

References

1. Chu, C.H., Huang, W.N. and Li, Y.W. "An integrated framework of tool path planning in five-axis machining of centrifugal impeller with split blades", *Journal of Intelligent Manufacturing*, **23**(3), pp. 687-98 (2012).
2. Xiao, J.M. and Zhao, C.M. "Key technology of five-axis NC programming and high-speed milling for integral impellers based on the general software UG", *Advanced Manufacturing Technology*, **314-316**(1-3), pp. 1633-1637 (2011).
3. Cho, M.H., Kim, D.W., Lee, C.G., Heo, E.Y., Ha, J.W. and Chen, F.F. "CBIMS: Case-based impeller machining strategy support system", *Robotics and Computer-Integrated Manufacturing*, **25**, pp. 980-985 (2009).
4. Fan, W.G., Wang, X.C., Cai, Y.L. and Jiang, H. "Rotary contact method for five-axis tool positioning", *Journal of Manufacturing Science and Engineering*, **134**(2), pp. 1087-1357 (2012).
5. Chaves, J.J., Poulachon, G. and Duc, E. "Optimal strategy for finishing impeller blades using five-axis machining", *International Journal of Advanced Manufacturing Technology*, **58**(5-8), pp. 573-583 (2012).
6. Jung, H.C., Hwang, J.D., Park, K.B. and Jung, Y.G. "A continuous control of cutter posture change for efficient five-axis machining of impeller", *Mechanical and Aerospace Engineering*, **110-116**(1-7), pp. 1619-1629 (2012).
7. Feng, J.R., Dai, X., Cheng, Y.Z. and Xiong, C.H. "Efficient tool path planning for machining an impeller with a five-axis NC machine", *Advanced Manufacturing Technology*, **156-157**(1), pp. 570-574 (2011).
8. Chen, X.B., Wang, J.B. and Xiong, Y.L. "Iso-scallop

- trajectory generation for the five-axis machining of an impeller”, *the 4th International Conference on Intelligent Robotics and Applications*, Aachen, Germany, pp. 487-94 (2011).
9. Huang, J.C., Liu, X.L., Yue, C.X., Cheng, Y.N. and Zhang, H. “Tool path planning of five-axis finishing milling machining for closed blisk”, *Materials Science Forum*, **723**, pp. 153-158 (2012).
 10. Gong, H. and Wang, N. “Five-axis flank milling free-form surfaces considering constraints”, *Computer Aided Design*, **43**(6), pp. 563-72 (2011).
 11. Chu, C.H., Wu, P.H. and Lei, W.T. “Tool path planning for five-axis flank milling of ruled surfaces considering CNC linear interpolation”, *Journal of Intelligent Manufacturing*, **23**(3), pp. 471-480 (2012).
 12. Beudaert, X., Pechard, P.Y. and Tournier, C. “Five-axis flank milling tool path smoothing based on kinematical behaviour analysis”, *Modelling of Machining Operations*, **223**, pp. 691-700 (2011).
 13. Beudaert, X., Pechard, P.Y. and Tournier, C. “Five-axis tool path smoothing based on drive constraints”, *International Journal of Machine Tools & Manufacture*, **51**(12), pp. 958-965 (2011).
 14. Layegh, S.E., Erdim, H. and Lazoglu, I. “Offline force control and feedrate scheduling for complex free form surfaces in five-axis milling”, *The Fifth Cirp Conference on High Performance Cutting*, Zurich Switzerland, **1**, pp. 96-101 (2012).

Biographies

Yuan Chen obtained BS and MS degrees in Mechanical Engineering from Hubei University of Technology, China, and a PhD degree in Mechanical Engineering from Harbin Institute of Technology, China. He is currently an Associate Professor in Shandong University at Weihai, China. His research interests are in the areas of parallel manipulator and NC technology, robotics, and motion control.

Guifu Mei received a BS degree in Mechanical Engineering from Shandong University of Science and Technology, and an MS degree in Mechanical Engineering from Shandong University at Weihai, China. He is currently a PhD student in Shandong University at Weihai, China. His main research interests are in the areas of NC technology.

Jiabin Wang. His biography was not available at the time of publication.

Chunyang Yao. His biography was not available at the time of publication.

Jun Gao received his MS and PhD degrees in Materials Science and Engineering from Shandong University, China. He is currently a Professor in Shandong University. His research interests are in the areas of materials plastic forming and intelligent control in materials processing.